International Journal of Remote Sensing

Modified light use efficiency model for assessment of carbon sequestration in grasslands of Kazakhstan: combining ground biomass data and remote-sensing

Pavel A. Propastin [a] , Martin W. Kappas [a] , Stefanie M. Herrmann [b] [c] & Compton J. Tucker [c]

[a] Department of Cartography, GIS & Remote Sensing, Georg-August-University Göttingen, 37077, Göttingen, Germany

[b] Space and Earth Science Research & Analysis, Science Systems and Applications Inc. (SSAI), Lanham, MD, 20706, USA

[c] Laboratory for Biospheric and Hydrospheric Processes, Biosphere Science Branch, NASA Goddard Space Flight Center, Greenbelt, MD, 20171, USA
Published online: 08 Nov 2011.

PLEASE SCROLL DOWN FOR ARTICLE

sources. The publisher shall not be liable for any loss, actions, claims, proceedings, demand, or costs or damages whatsoever or howsoever caused arising directly or indirectly in connection with or arising out of the use of this material.

Taylor & Francis
Taylor & Francis Group

Modified light use efficiency model for assessment of carbon sequestration in grasslands of Kazakhstan: combining ground biomass data and remote-sensing

PAVEL A. PROPASTIN*†, MARTIN W. KAPPAS†, STEFANIE M. HERRMANN‡§ and COMPTON J. TUCKER§

†Department of Cartography, GIS & Remote Sensing, Georg-August-University Göttingen, 37077 Göttingen, Germany

‡Space and Earth Science Research & Analysis, Science Systems and Applications Inc. (SSAI), Lanham, MD 20706, USA

§Laboratory for Biospheric and Hydrospheric Processes, Biosphere Science Branch, NASA Goddard Space Flight Center, Greenbelt, MD 20171, USA

A modified light use efficiency (LUE) model was tested in the grasslands of central Kazakhstan in terms of its ability to characterize spatial patterns and interannual dynamics of net primary production (NPP) at a regional scale. In this model, the LUE of the grassland biome (ε_n) was simulated from ground-based NPP measurements, absorbed photosynthetically active radiation (APAR) and meteorological observations using a new empirical approach. Using coarse-resolution satellite data from the Sea-viewing Wide Field-of-view Sensor (SeaWiFS), monthly NPP was calculated from 1998 to 2008 over a large grassland region in Kazakhstan. The modelling results were verified against scaled up plot-level observations of grassland biomass and another available NPP data set derived from a field study in a similar grassland biome. The results indicated the reliability of productivity estimates produced by the model for regional monitoring of grassland NPP. The method for simulation of ε_n suggested in this study can be used in grassland regions where no carbon flux measurements are accessible.

1. Introduction

The terrestrial carbon cycle is a highly dynamic system that includes several storage pools and flux components such as gross primary production (GPP) and net primary production (NPP). NPP is defined as the total photosynthetic gain of vegetation per unit ground area and per time unit, whereas GPP refers to the total amount of carbon that is fixed from the atmosphere by vegetation during photosynthesis. NPP is the difference between GPP and autotrophic photorespiration losses. In the past decades, ecosystem scientists have focused on the estimation of these key variables, which are indispensable for modelling net ecosystem exchange (NEE) between the atmosphere and ecosystems.

*Corresponding author. Email: ppropas@uni-goettingen.de

Two common approaches to estimate NPP are field measurements and satellite-based process models. The estimation of NPP by field methods involves the extensive *in situ* measurements of biomass, provided turnover of all components (e.g. aboveground, roots, understory, litter) is included (Rodin *et al.* 1975, Long *et al.* 1989, Roberts *et al.* 1993, Gower *et al.* 1999, Scurlock and Olson 2002). Generally, the ground-measured NPP is then defined as the rate of biomass growth (converted to carbon) within an assessment period, and the integrated sum of this growth over the growing period as annual NPP (Singh *et al.* 1975, Gower *et al.* 1999):

$$\text{NPP} = \sum P_i, \tag{1}$$

where P is the net production of dry biomass (recalculated to carbon) for each of the plant components i. For a given period of measurement, the NPP of a vegetation stand is equal to the change in both aboveground and belowground plant mass plus any loss over this period due to death and subsequent decomposition, herbivory and exudation/volatilization. Equation (1) is appropriate to calculate NPP for any ecosystem, although there are a number of estimation algorithms depending on the field measurement method chosen for a certain study. For short-stature ecosystems, such as grasslands, agricultural crops and tundra, area harvest is the most appropriate measurement method to estimate NPP in field (Singh *et al.* 1975, Scurlock and Olson 2002). The advantages and limitations of various methodologies have been reviewed in several published studies (Singh *et al.* 1975, Long *et al.* 1989, Roberts *et al.* 1993, Scurlock and Olson 2002).

Excellent measurements of NPP have been made in several studies for site-specific or stand-specific targets (Gower *et al.* 1999, Scurlock and Olson 2002). Despite their extensive usage, *in situ* measurements demand considerable amounts of work and time and yield information only for the close vicinity of the measured points. Such measurements can only obtain the local NPP value but cannot provide a NPP value over large areas. Scaling up data from ground NPP measurements is an important challenge for understanding the carbon cycle across different spatial scales and can be carried out using satellite-based empirical models linking spectral reflectance in satellite bands and ground-based values of NPP (Reich *et al.* 1999, Lu 2006).

Another approach to estimating GPP/NPP is to use the satellite-based light use efficiency (LUE) model, first described by Monsi and Saeki (1953) and extended by Monteith (1977), which links the incoming solar radiation to vegetation production through an empirical biophysical conversion factor (Running *et al.* 1999a, 2000, Seaquist *et al.* 2003, Xiao *et al.* 2004). The relationships between LUE and GPP/NPP are described by the following equations:

$$\text{GPP} = \varepsilon_g S \sum (\text{fPAR})(\text{PAR}), \tag{2}$$

$$\text{NPP} = \varepsilon_n S \sum (\text{fPAR})(\text{PAR}), \tag{3}$$

where PAR is the incident photosynthetically active radiation (MJ m^{-2}) for a time period; fPAR is the fraction of absorbed PAR by the vegetation canopy; ε_g is the LUE in the GPP calculation (g C MJ^{-1}); ε_n is the LUE in the NPP calculation (g C MJ^{-1}); and S is the environmental stress scalar. Both ε_g and ε_n are usually considered to be biome-specific constants (Gower *et al.* 1999, Ruimy *et al.* 1999, Singsaas *et al.* 2001),

the values of which are functions of the limiting climatic factors such as temperature, soil moisture and water vapour deficit.

LUE models were designed based on the assumption that plants use solar radiation for photosynthesis and assimilation of biomass. The amount of photosynthesis and biomass accumulated is related to LUE which is influenced by many factors. Monteith (1972) first developed the algorithm for NPP calculation using absorbed photosynthetically active radiation (APAR) and LUE. The Carnegie–Ames–Stanford approach (CASA) is the earliest simulation model using Monteith's approach for analysing global NPP. The global production efficiency model (GLOPEM) is another example that uses the LUE approach together with ecological processes.

In satellite-based LUE analysis, the amount of solar radiation reaching the canopy (PAR) is usually either derived from remotely sensed data or computed using mathematical algorithms (Frouin and Pinker 1995, Seaquist and Olsson 1999). Multispectral vegetation indices are commonly used to estimate fPAR from remotely sensed data (Asrar *et al*. 1984, Xiao *et al*. 2004). The normalized difference vegetation index (NDVI), computed from red (R) and near-infrared (NIR) satellite channels, has been most often used for the estimation of fPAR (Goward and Huemmrich 1992, Goward *et al*. 1994, Ruimy *et al*. 1994). Alternatively, fPAR can also be calculated as a function of the leaf area index (LAI) and light extinction coefficient (Ruimy *et al*. 1999).

LUE models are largely based on quantitative relationships between LAI and fPAR, or between NDVI and fPAR, and have been applied at regional to global scales using data from the Advanced Very High Resolution Radiometer (AVHRR) sensors (Field *et al*. 1995), the Sea-viewing Wide Field-of-view Sensor (SeaWiFS) (Behrenfeld *et al.* 2001), the Système Probatoire d'Observation de la Terre (SPOT) sensor (Xiao *et al*. 2004, Propastin and Kappas 2009a) and the Moderate Resolution Imaging Spectroradiometer (MODIS) sensor (Myneni *et al*. 1997, Running *et al*. 1999b, Running *et al*. 2000). Global estimations of NPP from AVHRR (GLOPEM) and MODIS data (MODIS NPP/GPP product) are freely available for public use. However, these products are not always appropriate for national or subregional studies, because the product algorithms incorporate a number of global biome-specific parameters, which ignore their inter-regional and within-region variability.

Field-measured NPP (equation (1)) is used as ground-truth information for validation of the satellite-based NPP models (equations (2) and (3)) in diverse biomes to ensure that the models accurately capture spatial patterns in NPP (Reich *et al*. 1999, Reeves *et al*. 2006, Fensholt *et al*. 2007). An extensive validation of MODIS NPP/GPP products is in progress using ground-truth data from different regions. The reported results of this validation revealed significant biome- and region-specific over-/underestimations of GPP/NPP (Justice *et al*. 2002, Fensholt *et al*. 2007). Therefore, for many regional and subregional studies, estimation of GPP/NPP using regionally and locally tuned parameters is preferable.

Developing and applying remote-sensing-based models for carbon sequestration has particular merit in data-impoverished regions of the world. One such region is the former Soviet Central Asia. Even though this region is economically disadvantaged, it is very rich in natural resources and has good prospects for socio-economic development. However, after the Soviet era this region has been out of the scope of remote-sensing research. The sophisticated remote-sensing-based monitoring that has become routine for accurately probing ecosystem processes in North America,

Europe and other intensively investigated regions has not yet been extended to Central Asia (Gilmanov *et al.* 2004, Henebry 2009). Kazakhstan is the region's largest country (2.7×10^6 km^2) with an area of more than 2×10^6 km^2 covered by different types of grassland. Although the production potentials of rangeland ecosystems are lower than those for other terrestrial ecosystems, grasslands of Kazakhstan have significant impact on the regional and global carbon cycles because of their expanse (Lioubimtseva *et al.* 2005). Grasslands also store a significant portion of their fixed carbon below ground, where it is resistant to fire effects (Lal 2004). Following the signing of the Kyoto Protocol by the Kazakhstan government in 2003, monitoring carbon sequestration over the huge territory of this republic has gained great scientific and political importance.

In this study, our aim is to design and test a modified LUE model using a new empirical approach for estimating the value of the LUE parameter (ε_n) based on ground measurements of grassland biomass. The modified LUE model was employed to simulate large-scale NPP dynamics in the grasslands of central Kazakhstan. Simulations of NPP were conducted using the 4.63 km spatial resolution data from the SeaWiFS over the period 1998–2008. The modelling results were verified against scaled NPP observations.

2. Study area

The study area is located in the central part of Kazakhstan between 48° 20′ and 49° 30′ N latitude and 72° and 74° 10′ E longitude. It encompasses the southern margin of the Kazakh Hills and the northern area of the Shetsky *raion* (district) in the Karaganda *oblast* (province). The climate of the region is dry, cold and highly continental. Average annual precipitation ranges from about 200 mm in the southern part to about 300 mm in the northern part of the study area, with an (interannual) coefficient of variation of 20–35% (Propastin 2007, pp. 61–69). The greater part of the precipitation falls during the warm period from March to October. The growing season starts in April and continues until October. The average July temperature is about 25–26°C.

Two main vegetation classes dominate the study area: short grassland, which covers 74.23% of the whole territory; and steppe grassland, which covers 25.77% (figure 1). Both grassland categories are dominated by the genera *Festuca* and *Stipa.* Few euryxerophilous forbs occur; the co-dominants are dwarf shrubs of the genus *Artemisia* and sometimes of other genera, particularly *Anabasis* and *Salsola*. The proportion of dwarf shrubs in the vegetation communities increases from steppe grassland to short grassland. Species diversity is about 12–15 species per square metre. The height of the canopy decreases from 30–40 cm in the north to 15–20 cm in the south of the study area, while vegetation cover decreases from 50–70% to 20–30%, and even less (Titlyanova 1988).

The vegetation growth in the study area is strongly dependent on precipitation dynamics. Grasses and shrubs grow during the whole vegetative period, but their growth is most rapid during May and early June (the period of greatest precipitation) in the southern part and during June in the northern part of the study area (Propastin 2007, pp. 72–79; Propastin *et al*. 2007). During the drier summer months (July and early August), their growth rate is slowed down. This period of semi-dormancy occurs throughout the study region.
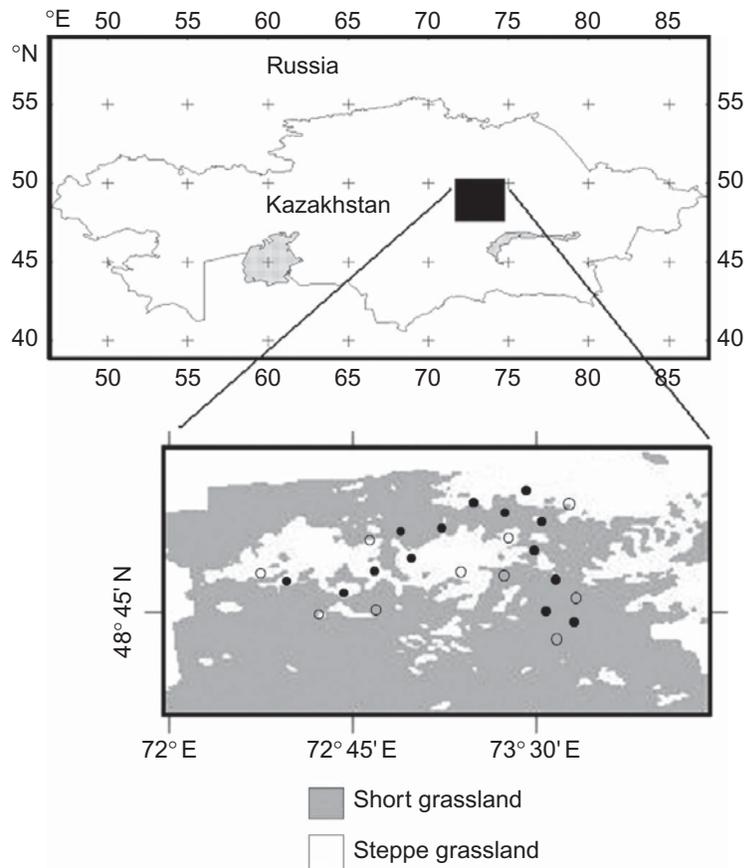
Figure 1. Location of the study region on a map of Kazakhstan and distribution of land cover classes in the study region based on the MODIS land cover map. Closed circles represent test sites where both biomass and vegetation structure were measured. Open circles represent sampling plots where only vegetation structure was measured.
Note: MODIS, Moderate Resolution Imaging Spectroradiometer.

3. Data sets and methodology

3.1 Satellite data

3.1.1 Satellite-based NDVI product. We used a satellite-based NDVI data set as input to our NPP model. The NDVI data set at 4.63 km spatial resolution covering the period 1998–2008 was obtained from the SeaWiFS (Tucker *et al.* in press). The NDVI was calculated from the R (660–680 nm) and NIR (845–885 nm) bands of SeaWiFS.

The SeaWiFS NDVI data are distributed as 30 day maximum value composites to minimize the effects of cloud contamination (Holben 1986) based on surface reflectances atmospherically corrected for Rayleigh and ozone effects. The compositing algorithm uses spatial homogeneity tests in the NIR band to maximize spatial coherence in addition to the maximum NDVI and minimum blue band criteria (Pinzon *et al.* 2001). Primarily designed as an ocean colour instrument, the SeaWiFS sensor requires highly accurate calibration, which is achieved by a spacecraft manoeuvre to scan the moon surface every lunar cycle for calibrating the sensor (lunar calibration) (Hooker *et al.* 1992). The resulting stability of its sensor measurements over time makes the SeaWiFS an excellent source of land data as well (Tucker *et al.* in press).

3.1.2 Landsat data. This study used two Landsat Enhanced Thematic Mapper Plus (ETM+) images (path 153/row 26) acquired on 19 June 2004 and 11 July 2008, respectively; both had level 1 G processing, a 30 m cell size. The preprocessing of both images included common steps for treatment of satellite data such as geometrical correction, geo-referencing and atmospheric correction. The images were geometrically corrected using a set of ground control points extracted from 1:100 000 topographic maps. The images were co-registered and projected to Universal Transverse Mercator (UTM) coordinates (World Geodetic System (WGS) 84 datum). The ETM+ digital numbers were transformed to reflectance values using ENVI 4.3 preprocessing function. The Landsat image from 19 June 2004 was used for deriving satellite-based models of LAI and fPAR, whereas the Landsat ETM+ image from 11 July 2008 was used for scaling up ground-based NPP observations.

3.2 Climate data

Ten-day temperature, air humidity and mean total cloud cover data for the period 1982–2008 at nine climate stations located in the study area were obtained from the National Hydrometeorological Centre of Kazakhstan. The 10 day values of the variables were averaged to monthly values for each of the nine climate stations and used for the generation of gridded maps. Gridded maps of mean monthly values for each variable were constructed using the interpolation method co-kriging, with a digital elevation model, scaled in metres, as a co-variable.

3.3 Field data collection

3.3.1 Sampling design. The study involved 14 test sites along a 200 km transect across the study area (figure 1), which were established by Space Research Institute of the Science Academy of Kazakhstan, as part of a research programme designed to measure long-term pasture production for the major land cover types in the district (Muratova 2007). Each of these test sites consists of a homogenous area with a size of several hectares. The location of the sites was selected to embrace a variety of geomorphological, hydrological and soil patterns explaining vegetation distribution throughout the district. Inside these test sites, field sampling plots for *in situ* measurements of biomass and vegetation structure (LAI and fPAR) were established. Additionally, outside the 14 test sites we established 11 sampling plots for measurements of vegetation structure.

3.3.2 Ground-based NPP. NPP of grassland was estimated from ground data on belowground and aboveground biomass collected at the 14 test sites at the peak of the growing season in June 2004. *In situ* measurements of biomass of standing crop (m_{AGB} = aboveground biomass) and litter matter (m_L = litter biomass) were conducted with several replicates per site. The peak season m_{AGB} and m_L were measured by destructive sampling of 1.0 m^2, with samples dried and weighed at 65°C to constant weight to correct for moisture content. Root biomass (m_{BGB} = belowground biomass) was collected at each test site with four replicates by excavating a square of 1 m × 1 m to a depth of 50 cm. The root matter was washed of soil and mineral contamination, dried at 65°C and weighed. The original values of dry matter were converted to carbon (g C m^{-2}) through multiplication with the carbon proportion factor of 0.47 (Tyurmenco 1975).

All published methods for NPP estimation from ground-measured biomass in grasslands can be grouped under seven algorithms as outlined in Scurlock and Olson (2002). From these seven algorithms, peak aboveground biomass algorithms are commonly used for estimation of NPP in grasslands where only one or two measurements per year are available (Singh *et al*. 1975, Long *et al*. 1989, Scurlock and Olson 2002). Sometimes conversion factors have been applied to estimate the ratio of belowground to aboveground production. The basic assumption of the peak biomass algorithms is that any live biomass was formed in the current year and any standing dead matter was formed by death in current year (Singh *et al*. 1975, Long *et al*. 1989, Scurlock and Olson 2002). Similar assumptions about complete plant mortality in grasslands underlie parameterization of the BIOME-BioGeochemical Cycles (BIOME-BGC) (White *et al*. 2000) and the MODIS NPP/GPP algorithms (Heinsch *et al*. 2003). The peak biomass algorithms are particularly appropriate in temperate grasslands, where the carbon pools in living aboveground biomass are turned over every year. But the major error source does not account for roots turnover and biomass (contained in litter) carried over from previous year (Long *et al*. 1989, Scurlock and Olson 2002).

In this study, we expanded the peak aboveground biomass algorithm (Singh *et al*. 1975, Long *et al*. 1989) by incorporating belowground and litter compartments. In the expanding algorithm, we considered roots turnover and biomass carried over from previous year:

$$\text{NPP} = m_{\text{AGB}} + m_{\text{L}} r_{\text{decom}} + m_{\text{BGB}} r_{\text{turnover}}, \qquad (4)$$

where r_{decom} is the relative rate of decomposition for litter and r_{turnover} is the turnover rate of roots. The underlying assumptions are the same as for the common peak aboveground biomass algorithm, but some litter and belowground biomass parts were carried over from the previous year. The relative decomposition rate of litter for grasslands (0.85) was calculated using data given by Zhang *et al.* (2008). Belowground production of current year was considered by imposing a conversion factor of 0.3 as the turnover rate of fine roots for the temperate grassland biome as in the BIOME-BGC algorithm (White *et al*. 2000).

3.3.3 LAI estimations. *In situ* measurements of LAI and fPAR were carried out at sampling plots established inside each of the 14 test sites and at the 11 additional sampling plots outside the test sites. In all cases, the plot size for LAI and fPAR measurements was chosen to correspond to an area observed by 3 × 3 Landsat ETM+ pixels (McCoy 2005). Each plot had a size of 90 × 90 m². The measurements were made in a 30 m transect spacing within each plot. In total 14 measurements were completed within each of the sampling plots, which were then averaged to mean values over corresponding plots.

An optical method was used in this study to acquire ground-based LAI and fPAR data for remote-sensing algorithm development. Hemispherical photography was performed using a WinScanopy Image Acquisition instrument developed by REGENT INSTRUMENTS, Toronto, ON, Canada (http://www.regentinstruments.com). The CanEye software (INRA, d'Avignon, France, www4.paca.inra.fr/emmah_eng/.../ Production.../CAN-EYE) was employed for the processing of hemispherical photographs. Gap fraction, the proportion of unobstructed sky, was calculated at 5° zenith angle intervals and used for additional calculations. LAI, fPAR and other vegetation

structure indices were calculated using routine procedures included in the CanEye software. Calculating formulae and operation of CanEye are described in detail in the CanEye manuals (CanEye manuals 2006) following the methods described by Jonckheere *et al.* (2004) and Weiss *et al.* (2004).

CanEye computes LAI based on the use of a lookup table derived using the Poisson model, that is, a reference table composed of gap fraction value in different view zenith angles and the corresponding LAI and average leaf angle parameters using an ellipsoidal leaf inclination distribution. The effective LAI is computed assuming random foliage element distribution. The true LAI is corrected for non-random distribution of foliage elements based on the clumping index, which is calculated using the logarithmic gap averaging technique given by Lang and Xiang (1986).

The CanEye-derived actual fPAR was calculated as the sum of two terms, weighted by the diffuse fraction in the PAR domain: the 'black sky' fPAR that corresponds to the direct component at a given solar position (date, hour and latitude) and the 'white sky' (or diffuse) fPAR. The 'black sky' fPAR, $fPAR^{BS}$, is approximated at each solar hour as the gap fraction (P_0) and the corresponding solar zenith angle (θ_s):

$$fPAR^{BS}(\theta_s) = P_0(\theta_s). \tag{5}$$

The 'white sky' fPAR, $fPAR^{WS}$, is computed as follows:

$$fPAR^{WS} = 2 \int_0^{\frac{\pi}{2}} P_0(\theta_s) \cos \theta_s \sin \theta_s d(\theta_s). \tag{6}$$

CanEye-derived LAI and fPAR values for individual subplots were averaged to generate per-site values. The calculated per-site LAI ranges from 0.19 to 1.78 with a mean value of 0.71, while the per-site fPAR ranges from 0.18 to 0.41 with a mean value of 0.27. The produced ground-based LAI and fPAR data sets were then used for developing a satellite-based LAI/fPAR data set.

3.4 *Scaling up field observations*

3.4.1 Scaling ground-based NPP. Ground-based NPP observations were spatially scaled (aggregated) for comparison with the SeaWiFS-based modelled NPP by relating NPP values recorded at the 14 test sites to spectral reflectance in Landsat ETM+ data. A detailed description of the NPP scaling is given in the study by Propastin and Kappas (2010). Here, we give only a brief explanation. The Landsat ETM+ image acquired on 17 June 2004 was used to determine the spectral response of grassland vegetation for creation of the NPP scaling model. A series of statistical tests were performed to establish the most robust relationship between ground-based NPP measurements and Landsat ETM+ reflectance. These tests included simple and multiple regressions using spectral reflectance in the individual Landsat bands and Landsat-derived vegetation indices. When extracting spectral Landsat reflectance values, we tested different aggregation levels from 3 pixels × 3 pixels kernel placed over each individual test site to averaging within each of the 14 test sites. Ordinary least squares method was used to evaluate statistical significance and the accuracy of the regression

relationship between ground-based NPP and Landsat reflectance. The best accuracy model for NPP scaling was produced by employment of the NIR-corrected NDVI ($NDVI_c$; see Brown *et al.* (2000)). This model explained more than 70% of the total variance in the ground-based NPP and showed a root mean squared error (RMSE) of 43.61 g C m^{-2} (Propastin and Kappas 2010):

$$NPP = 876.72(NDVI)_c - 1.949. \tag{7}$$

Equation (7) was employed to the Landsat ETM+ scene to create a fine-resolution NPP map over the study area.

3.4.2 Scaling ground-based fPAR observations. Recent studies have proved that fPAR is closely related to NDVI. The latter can be converted into fPAR by means of the fPAR/NDVI relationship, the parameters of which are independent of the vegetation cover heterogeneity of the pixel (Myneni and Williams 1994, Ruimy *et al.* 1999). For a range of non-woody vegetation types, this relationship has been found to be remarkably consistent. However, the fPAR/NDVI relationship is very sensitive to soil reflectance and differences in sun/sensor geometry. The linear relationship for fPAR is valid only for satellite data which are corrected for atmospheric and bidirectional effects, and background contributions to the signal must be accounted for (Myneni and Williams 1994). Otherwise, a different model, for example, asymptotic, can be used. Since bidirectional effects and background contributions to the signal were not considered in the SeaWiFS NDVI data set in this study, we used a non-linear regression model between fPAR and NDVI.

The Landsat ETM+ image acquired on 11 July 2008 was used to determine an NDVI-based model for further use with the SeaWiFS NDVI data. The model was calibrated based on the ground fPAR values obtained from hemispherical photography (§3.3.3) and the corresponding NDVI was recorded on the 25 sampling plots:

$$fPAR = 2.3193(NDVI)^{2.1302}. \tag{8}$$

The model was statistically significant at the level of $p < 0.01$ with the value of the coefficient of determination $R^2 = 0.61$ (RMSE = 0.10). This model was further used to calculate monthly fPAR for the period 1998–2008 for the SeaWiFS data set.

4. Description of the SeaWiFS-based NPP algorithm

Figure 2 shows the generalized processing stream in the NPP model. The parameters inside the ellipsoids represent the raw data used in the model, whereas the parameters inside the boxes are derived during the execution of the model. A detailed description of the individual parameters, modelling steps and equations is presented in a flowchart as follows.

4.1 *Modelling photosynthetically active radiation*

The PAR is defined as the domain of incoming solar radiation exploited by green vegetation for photosynthesis (400–700 nm). Since no ground measurements of solar radiation are available for the study area, PAR was obtained on a pixel-by-pixel basis
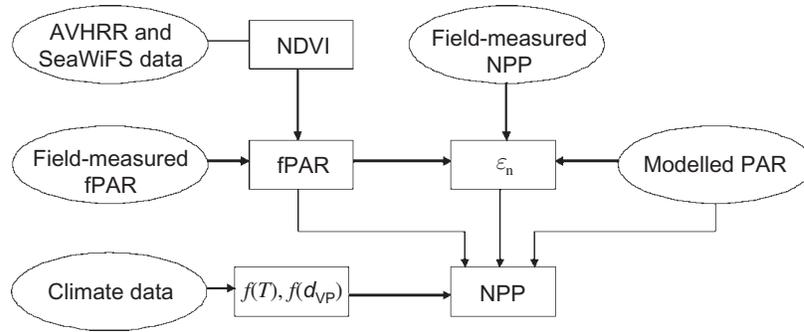
Figure 2. Flowchart of the LUE model developed in this study.
Note: LUE, light use efficiency; AVHRR, Advanced Very High Resolution Radiometer; SeaWiFS, Sea-viewing Wide Field-of-view Sensor; NDVI, normalized difference vegetation index; NPP, net primary production; PAR, photosynthetically active radiation; fPAR, fraction of absorbed PAR; ε_n, the LUE in the NPP; T, the effect of temperature; d_{VP}, the effect of vapour pressure deficit (VPD).

from the budget modelling approach, which computes the solar irradiance at the top of the atmosphere and transforms it into the amount of solar radiance reaching the Earth's surface. The modelling approach calculates the solar radiance at the top of the atmosphere as a function of the following variables: Earth–Sun distance, solar inclination, the angle between the Earth's orbital and equatorial planes, solar elevation angle, geographical position and day of year (Monteith and Usworth 1990). The variables of surface elevation, day length and mean total cloud cover information were used to compute optical depth of the atmosphere and to estimate solar irradiance reaching the ground. Spatial distribution of the radiation reaching the ground strongly depends on the terrain geometry of (relief slope, exposition, aspect). These variables were obtained from a digital terrain model and used as input to the equation given by Alisov *et al.* (1956). The incoming solar energy is reduced to PAR assuming a ratio of PAR to global radiation of 0.48 (Begue *et al.* 1991, Frouin and Pinker 1995). The amount of the APAR was calculated through multiplication of PAR with fPAR.

4.2   *LUE parameter*

The LUE varies with vegetation types, and information about its values for individual vegetation types is summarized in several publications (Ruimy *et al.* 1995, Gower *et al.* 1999, Singsaas *et al.* 2001). The empirical method to estimate a value of LUE is to analyse the response of the vegetation photosynthetic rate to the incident solar radiation absorbed by plants. Estimation of the ε_n parameter is commonly based on the use of data from measurements of carbon dioxide (CO_2) flux and photosynthetic photon flux density (Ruimy *et al.* 1999). Alternatively, the LUE can be calculated using ground-based biomass measurements and the amount of PAR absorbed by vegetation (Propastin and Kappas 2009b). Through conversing equation (3), the parameter ε_n may be calculated as follows:

$$\varepsilon_n = \frac{(\text{NPP})}{S \sum_{i=1}^{k} (\text{fPAR}_i)(\text{PAR}_i)}, \tag{9}$$

where k is the length of the growing season; i represents shorter periods (days, weeks or months) within the growing season; PAR_i is the incident photosynthetically active radiation ($MJ\,m^{-2}$) for a short period i; and $fPAR_i$ is the fraction of absorbed PAR by the vegetation canopy for the period i. Replacing NPP in equation (8) with equation (4) leads to

$$\varepsilon_n = \frac{m_{AGB} + m_L r_{decom} + m_{BGB} r_{turnover}}{S \sum_{i=1}^{k} (fPAR_i)(PAR_i)}, \tag{10}$$

where S is the environment stress scalar and k is the length of the growing season (in this study – in months).

The value of ε_n is suggested to be a biome-specific constant, which can be used in similarly composed ecosystems (Ruimy *et al.* 1995, Gower *et al.* 1999, Singsaas *et al.* 2001). This uniformity facilitates scaling up ground measurements of NPP to cover entire regions dominated by grasslands.

4.3 *Climatic determinants of LUE*

LUE is affected by environmental conditions, particularly temperature and water availability, whose effects can be modelled using simple functions (White *et al.* 2000, Turner *et al.* 2003):

$$S = f(T)f(d_{VP}), \tag{11}$$

where S is the environmental stress scalar; T and d_{VP} are the scalars for the effects of temperature and vapour pressure deficit (VPD), respectively.

In this study, T is simulated at each time step using the equation developed for the terrestrial ecosystem model (Reich *et al.* 1999):

$$f(T) = \frac{(T - T_{min})(T - T_{max})}{(T - T_{min})(T - T_{max}) - (T - T_{opt})^2}, \tag{12}$$

where T_{min}, T_{max} and T_{opt} are the minimum, maximum and optimal temperatures for photosynthetic activity, respectively. The values for the temperature parameters were taken from White *et al.* (2000). If air temperature falls below T_{min}, $f(T)$ is set to 0.

The effect of water on plant photosynthesis has been estimated as a function of soil moisture or water VPD in a number of satellite-based LUE models (Field *et al.* 1995, Running *et al.* 2000, Seaquist *et al.* 2003). The d_{VP} index scales the availability of atmospheric moisture between the values at which the photosynthesis process stops and the optimum value corresponding to each vegetation type. The d_{VP} function is expressed as

$$f(d_{VP}) = \begin{cases} 0 & d_{VP} > d_{VP}^{stop} \\ (d_{VP}^{stop} - d_{VP})/(d_{VP}^{stop} - d_{VP}^{start}) & d_{VP}^{start} < d_{VP} < d_{VP}^{stop} \\ 1 & d_{VP} < d_{VP}^{stop} \end{cases} . \tag{13}$$

The values for minimum, maximum and optimum of VPD parameters were taken from BIOME-BGC (White *et al*. 2000).

4.4   *Model evaluation*

After simulation of the model parameters, we calculated SeaWiFS-based NPP for the study area. The model was run with a resolution of 4.63 km, time steps of 30 days and time span from 1998 to 2008 using the SeaWiFS NDVI data set as input. In general, the evaluation of a regional modelling approach is difficult. This holds especially true for the research area in central Kazakhstan. Commonly, CO_2 flux data from eddy covariance measurements are used for evaluation of satellite-based LUE models (Running *et al*. 1999a). Unfortunately, there are no accessible eddy flux data from this region. Another evaluation strategy is to compare spatial patterns of satellite-simulated NPP data with biomass values measured at sampling plots (Reeves *et al*. 2006, Fensholt *et al*. 2007). However, a direct comparison of ground data with a coarse-resolution product cannot be efficient, because the pixel scale of such a product is much coarser than a sampling plot's scale and the results of such a comparison would be poor. In this case, biomass values measured at individual plots can be scaled up using a fine-resolution satellite image and after that compared with the coarse-resolution product (Reich *et al*. 1999, Running *et al*. 1999a, McCoy 2005, Reeves *et al*. 2006).

While the research process is still going on, three types of evaluation of the resulting data were accomplished in this study. First, modelling results were compared with data from the literature. Second, the modelling results were evaluated against the ground-based NPP data from the 14 sampling sites in the study area with respect to spatial consistency. Because of scale difference between the ground data and SeaWiFS pixel size, we compared the SeaWiFS NPP retrieval with the Landsat ETM+ NPP estimation (from equation (7)), which was aggregated to a 4.63 km resolution of SeaWiFS. The second one was used as ground reference for the assessment of the SeaWiFS-derived product of NPP. Further, we computed frequency distributions of the obtained SeaWiFS-based NPP and compared them with the scaled NPP. In order to examine the correspondence of distribution histograms, we used the *F*-statistics to test the null hypothesis that the frequency distribution of two data sets is similar.

Finally, the modelled NPP data set was compared with the independent ground-based NPP data set from the Shortandy grassland study site (Shatokhina 1988, Gilmanov 1996) with respect to temporal consistency. This data set was used in a number of recent studies to validate models of vegetation–soil–atmosphere interactions (Gilmanov *et al*. 1997) and compile global NPP data sets (Scurlock and Olson 2002, Hui and Jackson 2006).

5.   Results

5.1   *Calibration of the NPP model*

5.1.1   Ground-based NPP.   Figure 3 shows the biomass of different ecosystem compartments and the NPP measured for the 14 test sites. The NPP ranges from 58.9 to 288.4 g C m^{-2}, indicating an SD of 68.6 g C m^{-2}. The mean NPP of all 14 sample plots was 152 g C m^{-2} showing a variability of 44% between the individual sample plots. The living aboveground biomass (m_{AGB}) together with litter (m_L) represents the largest carbon pool, whereas the belowground part (m_{BGB}) contains about 23% of carbon (33.6

Table 1. Previous estimates of primary production (GPP and NPP) in arid and semi-arid zones.

Location and vegetation type	Estimating technique	GPP $(g\ C\ m^{-2})$	NPP $(g\ C\ m^{-2})$	References
Central Asia	Field observations			
Dry steppe			326	Perschina and Yakovlewa
Dry steppe			126	(1960), Makarowa (1971),
Dry steppe			148	Gristchenco (1972),
Semi-desert			90–310	Tyurmenco (1975),
Semi-desert			117–189	Fartuschina (1986) and
Semi-desert			220	Robinson *et al.* (2002)
Semi-desert			114	
Former Czechoslovakia	Field observations			
Grassland		664	481	Tesarova and Gloser
Grassland		492	318	(1976) and Rychnovska
Global	Field observations			*et al.* (1980)
Grassland			70–410	Zheng *et al.* (2003) and
Grassland			91–385	Rodin *et al.* (1975)
Wyoming, USA	Measurements of net ecosystem exchange			
Mixed-grass prairie		321		Hunt *et al.* (2004)
Sagebrush steppe		239		
Sahel, Niger Grassland	Satellite-based LUE model	352	169	Seaquist *et al.* (2003)
Central Kazakhstan	Satellite-based LUE model			
Dry steppe		243	145	Propastin and Kappas
Short grassland		211	131	(2009a)

Note: GPP, gross primary production; NPP, net primary production; LUE, light use efficiency.

g C m^{-2}) from the total amount. With regard to the previously published studies on ground-based NPP measurements in grasslands (see table 1), the ground-measured values of NPP from this study are well within the range of NPP reported from Central Asia and other dryland regions. The compilations of the studies from Central Asia have defined the known range of NPP in the dry steppe biome from 126 to 326 g C m^{-2} year^{-1} (Perschina and Yakovlewa 1960, Makarowa 1971, Tyurmenco 1975) and in short grassland from 114 to 220 g C m^{-2} year^{-1} (Fartuschina 1986, Robinson *et al.* 2002). These values are highly consistent with the values obtained in this study. The results of this study go well with the scope of NPP values averaged globally for grassland biomes (Rodin *et al.* 1975, Scurlock and Olson 2002, Zheng *et al.* 2003).

5.1.2 Light use efficiency. For each of the 14 NPP test plots, a value of ε_n was calculated using equation (10). The obtained ε_n values ranged from 0.51 to 0.95 g C MJ^{-1} with a mean value of 0.72 g C MJ^{-1} and an SD of 0.21 g C MJ^{-1} and are well within the range of reported ε_n values for grassland biomes in other world regions (Ruimy *et al.* 1995, Gower *et al.* 1999, Singsaas *et al.* 2001, Hill *et al.* 2004). The mean ε_n
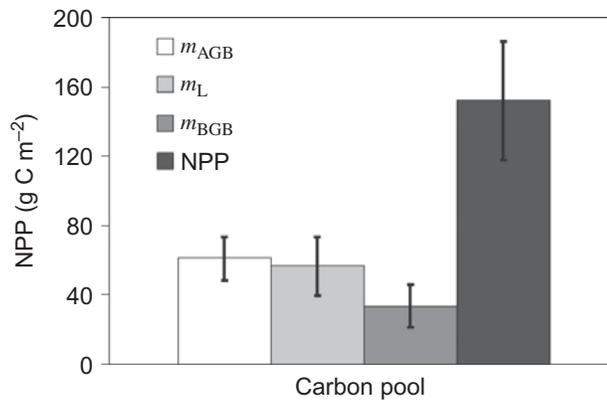
Figure 3.   Mean NPP of different ecosystem parts and the total NPP measured at 14 test sites in grassland of central Kazakhstan. Whiskers represent the SD.
Note: m_{AGB}, aboveground biomass; m_L, litter biomass; m_{BGB}, belowground biomass; NPP, net primary production; SD, standard deviation.

value from this study is very close to the value proposed by Potter *et al.* (1993) as the universal LUE for estimating worldwide NPP in CASA model. For comparison, the ε_n value used in the MODIS algorithm is 0.68 g C MJ^{-1} (Heinsch *et al.* 2003).

Particularly important is the comparison of the ε_n value from this study with LUE used for modelling NPP of analogous grassland ecosystems of Central Asia and other regions. Thus, Jinguo *et al.* (2006) found an ε_n value of 0.39 g C MJ^{-1} to be fairly adequate for estimation of NPP over a short grassland region in the northern Hebei Province of China, whereas Yuan *et al.* (2008) used an ε_n value of 0.61 g C MJ^{-1} for modelling NPP of a mixed grassland in northern Tibet. Hill *et al.* (2004) empirically determined a value of $\varepsilon_n = 0.85$ for grassland pastures in Australia. The study by Gilmanov *et al.* (2004) found a LUE of GPP, $\varepsilon_n = 2.17$ g C MJ^{-1}, for a tall grassland ecosystem in northern Kazakhstan. The value of ε_g reported by Gilmanov *et al.* (2004) is relatively high and is only slightly lower than the value of LUE for GPP suggested by Ruimy *et al.* (1995) as the upper limit for grasslands. When we suggest that autotrophic respiration of a grassland ecosystem is equal to about 50% of GPP, the ε_n from the study by Gilmanov *et al.* (2004) would have a value of about 1.08 g C MJ^{-1}. This value would be a threshold in the ε_n value range compiled by Gower *et al.* (1999), whereas the value of 0.72 g C MJ^{-1} from this study is in the centre of the range of ε_n values.

This shows that the empirical method used for estimation of the ε_n parameter in this study worked very effectively and the obtained mean ε_n value is appropriate to be employed for scaling up NPP of grassland over the study area.

5.2   *Outputs from the SeaWiFS-based NPP model*

The LUE model is used to calculate NPP at a spatial resolution of 4.63 km and a temporal resolution of 1 month over the study region. Spatial distribution of the SeaWiFS-simulated NPP for 2004 is shown in figure 4(*a*). For comparison, the Landsat-derived NPP at a 30 m spatial resolution is shown in figure 4(*b*). The SeaWiFS NPP estimates varied spatially in a similar pattern to that of the Landsat-scaled NPP, even though the patterns in scaled NPP are much finer. For the SeaWiFS simulation, the annual NPP ranged from 64 to 302 g C m^{-2} with a mean NPP of 168 g C m^{-2} and

the SD was 53 g C m^{-2}. The Landsat-scaled NPP ranged from 66 to 253 g C m^{-2} and showed somewhat lower value of the mean NPP and somewhat larger SD: 161 and 53 g C m^{-2}, respectively.

There is a distinct south–north gradient in NPP distribution over the study region. The distribution of NPP over the study area agrees with expectations on NPP geographical distribution with respect to climate patterns. In general, the mapped NPP patterns reflect the temperature and precipitation gradients observed in the study area. The southern areas show low biomass production with NPP values of 100–120 g C m^{-2}, while the northern areas demonstrate much higher NPP with values above 200 g C m^{-2}. This pattern is driven primarily by the distribution of precipitation that changes from about 250–280 mm in the north to about 150–180 mm in the south of the study area. Correspondingly, the mean summer temperature increases significantly from north to south leading to a more prolonged semi-dormancy phase of vegetation during July–August in the south of the study area (Propastin *et al*. 2007).

The annual product as shown in figure 4(*a*) is the sum of monthly NPP values for 2004. Monthly time series of the SeaWiFS-simulated NPP for two sites located in short grassland and dry steppe is shown in figure 5. Within temperate grasslands of Central Asia, the principal mode of variability in vegetation productivity is generally associated with seasonality of climatic factors. The vegetation growth starts when mean temperature rises above 0. In the study area, this occurs in the first/second decades of April. The vegetation growth achieves its maximum in late June to early July and decreases persistently during the rest of the growing season. The climate-dependent seasonal dynamics of vegetation production are captured reasonably well by the model simulation.

In both vegetation types, plant growth starts in April when air temperature rises above 0 (figure 5). However, NPP at the short grassland site increases more rapidly than at the dry steppe site. At the short grassland site, the maximum monthly NPP is commonly achieved in June, whereas the dry steppe grassland site demonstrates the NPP peak in July despite the fact that maximum precipitation in the study region occurs in early June. A reason for this is the delayed response of vegetation to precipitation which amounts to 30–40 days as reported for steppe grassland in the study region (Propastin *et al*. 2007). The NPP at the short grassland site decreased earlier than at the dry steppe site, reflecting the earlier senescence of herbaceous vegetation due to drought-like conditions caused by the decreased precipitation and high temperatures in July–August. These conditions raise respiration rates, which considerably
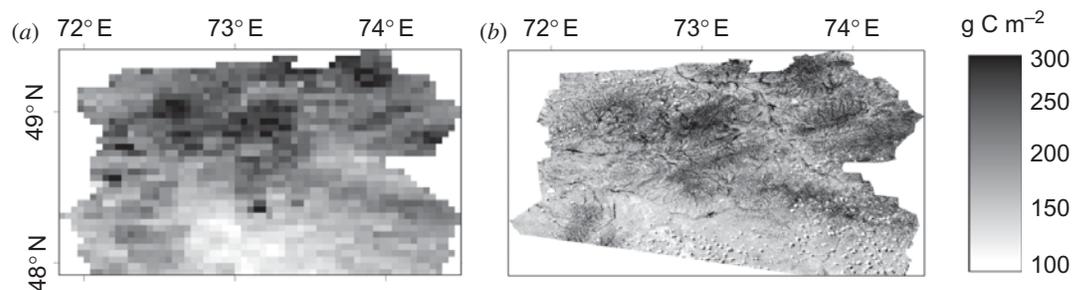

Figure 4. Spatial distribution of the study area's NPP simulated using (*a*) the 4.63 km SeaWiFS data for 2004 and (*b*) the Landsat-scaled NPP at a 30 m spatial resolution.
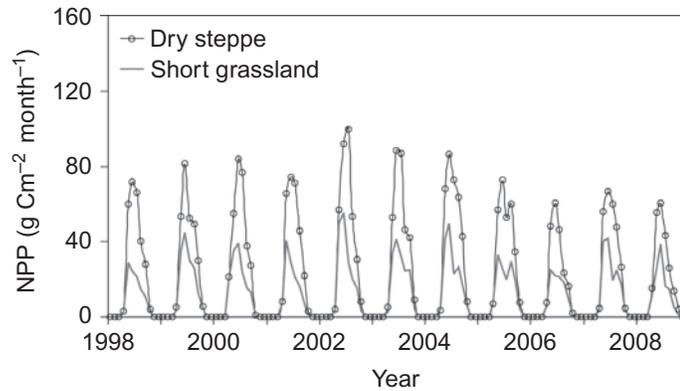Note: NPP, net primary production; SeaWiFS, Sea-viewing Wide Field-of-view Sensor.

Figure 5. Seasonal dynamics of monthly NPP simulated from the SeaWiFS model for dry steppe and short grassland.
Note: NPP, net primary production; SeaWiFS, Sea-viewing Wide Field-of-view Sensor.

decrease the carbon sequestration by grass vegetation. During the summer months, the short grassland site generally had lower monthly NPP than the dry steppe site, which is characterized by the more favourable climatic conditions. Thus, the mean monthly NPP for July amounts to 83 g C m^{-2} for the steppe site and 51 g C m^{-2} for the short grassland site. At the beginning and end of the growing season (April and October), monthly NPP values for both vegetation types are similar.

5.3 *Validation of the modelling results*

A direct comparison of the modelling results with the ground-based NPP estimations for the 14 test sites is problematic because of a mismatch in the spatial resolution of the SeaWiFS data versus the sampling sites. The validity of the coarse-resolution NPP data can be investigated by the analysis of the frequency distribution of NPP values and their consistency with the Landsat-scaled NPP. Another strategy is a pixel-by-pixel comparison of the SeaWiFS NPP with the fine-resolution Landsat NPP aggregated to the SeaWiFS pixel resolution. In this work, both strategies were employed for the investigation of the validity of the SeaWiFS NPP.

A histogram of NPP values at 4.63 km resolution shows similar trends to that observed at 30 m resolution (figure 6), even though a comparison between trends presented for the SeaWiFS NPP shows a small shift to higher values of NPP. The F-test was carried out in order to examine whether the frequency distributions of the Landsat-scaled NPP at 30 m and the SeaWiFS-simulated NPP at 4.63 km resolution are similar. The F-test results proved the similarity of frequency distribution at the p-level < 0.05.

The Landsat-scaled NPP was aggregated to a 4.63 km resolution and compared with the SeaWiFS NPP in figure 7. Both NPP data sets show significant correlation ($p < 0.05$) at the pixel level ($R^2 = 0.75$, RMSE = 26.6 g C m^{-2}). The results reveal a high consistency of the NPP modelled by the SeaWiFS-based model with the Landsat-scaled NPP. However, the results also show that the SeaWiFS NPP product has a slight trend to higher values in comparison with the Landsat NPP. The SeaWiFS NPP slightly underestimates lower NPP values in comparison with the Landsat NPP product and overestimates higher NPP values. The reason for this may be that spatial resolution increases the homogeneity of the area covered by a larger pixel exposing a lower spatial variance of the NPP variable.
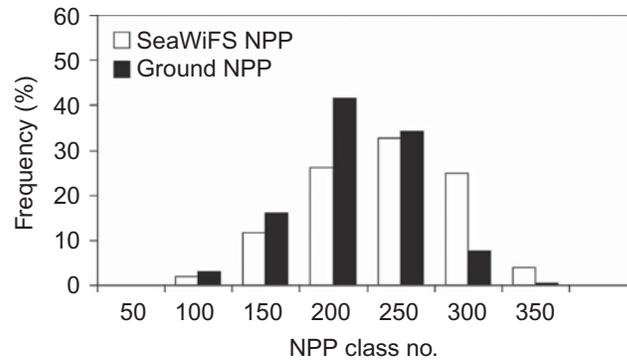
Figure 6.   Histograms of the NPP simulated by the 4.63 km SeaWiFS and the 30 m Landsat scaled NPP.
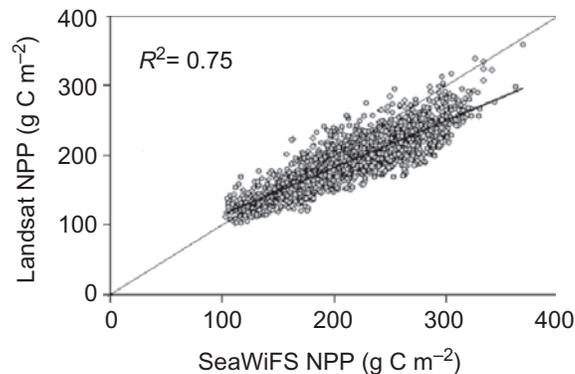Note: NPP, net primary production; SeaWiFS, Sea-viewing Wide Field-of-view Sensor.

Figure 7.   Comparison of the NPP simulated using the SeaWiFS data versus the Landsat-scaled NPP aggregated to 4.63 km.
Note: NPP, net primary production; SeaWiFS, Sea-viewing Wide Field-of-view Sensor.

The SeaWiFS-simulated monthly NPP values for the study period 1998–2008 were merged into averaged monthly time series and compared with long-term averaged monthly NPP from a similar grassland environment in Shortandy, Kazakhstan (Shatokhina 1988, Gilmanov 1996). The Shortandy grassland site (51.0° N and 71.2° E) had an average annual precipitation of 330 mm and had species composition similar to that of the dry steppe grassland in the current study area. Comparison of the Shortandy NPP with the SeaWiFS-simulated data showed good agreement in terms of seasonality and NPP values for individual months (figure 8). There was good agreement with regard to the beginning and end of the growing season. The seasonal maximum value in both data sets occurred in June. Statistical tests proved that the relationship between these data sets was very strong and statistically significant at $p < 0.0001$ level ($R^2 = 0.91$). The RMSE was 15.08 g C m^{-2} month^{-1} (12% of the mean monthly value). There was a little negative bias (6.2 g C m^{-2} month^{-1}) between simulations and Shortandy NPP observations in the mean monthly NPP value. The maximum for the SeaWiFS product was 106 g C m^{-2} month^{-1}, about 8 g C m^{-2} month^{-1} lower than the maximum value at the Shortandy site. The reason for this is a higher precipitation amount at the test site of Shortandy in comparison with the dry steppe grassland in the study area.
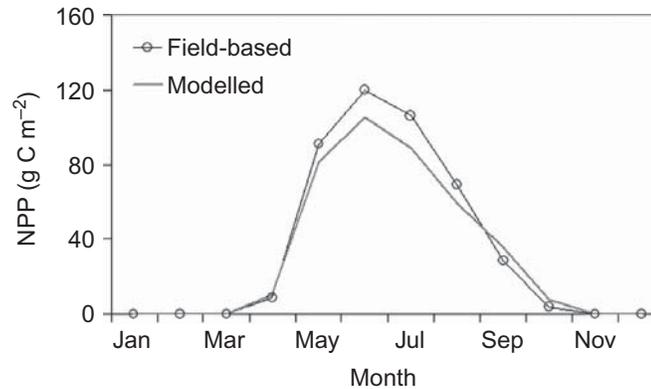
Figure 8.   Monthly variations of ground-based NPP at the Shortandy test site (thin line with circles) and dry steppe NPP modelled in this study (thick line).
Note: NPP, net primary production.

6. Conclusion

This study presented an algorithm for remote estimation of NPP over a grassland region in central Kazakhstan using ground data of aboveground/belowground grass biomass and vegetation structure parameters collected from field sites, climatic data and time series of coarse-resolution SeaWiFS (4.63 km) data. This study used the well-known Monteith LUE approach (Monteith 1977), but the most important advantage of the model presented is the exclusive use of the variables obtained from field survey data for calibration and validation of the model. While our model is similar to some others to the extent that it is embedded in a LUE framework (e.g. Field *et al*. 1995, Seaquist *et al*. 2003, Hill *et al*. 2004), our approach differs from others in that it uses a new technique for estimation of the LUE parameter. This technique relates the PAR absorbed by plants to the total NPP estimated from the field-measured peak aboveground and belowground biomass. In comparison with the common techniques for estimation of the LUE, such as the analysis of CO_2 flux and photosynthetic photon flux density, which demand time-consuming measurements using complex and expensive equipment (Running *et al*. 1999a, Xiao *et al*. 2004), the technique used in this study is relatively simple but very effective. Our research shows that this parameterization of LUE is both pragmatic (given the deficiency of CO_2 flux data from the study area) and biophysically realistic, as the value of LUE estimated by this approach highly coincides with values reported in recent literature from grassland biomes in Central Asia and other regions (Potter *et al*. 1993, Ruimy *et al*. 1995, Gower *et al*. 1999, Hill *et al*. 2004).

To the extent possible, we have compared our derived NPP with ground-measured NPP data to ensure that our model performed in a robust manner. This was of major concern because a direct comparison of the modelling results with the ground-based NPP for the 14 test sites was possible only with a strong stipulation for the significant differences between the spatial unit size of the ground measurements and the coarse resolution of the satellite sensors. For this reason, we used a Landsat ETM+ image for scaling up ground NPP. The Landsat scaled NPP map was then used as ground truth for evaluation of the SeaWiFS-based NPP product. The evaluation results detected tight association between the scaled NPP and the modelled NPP.

The estimates of the model were also evaluated with respect to temporal consistency using a ground-based NPP data set from a similar grassland environment in northern Kazakhstan (the Shortandy site). The monthly NPP product derived in this study was very close to the ground-based NPP considering all phases of the growing period. Taking into consideration all the results of the evaluation tests undertaken in the study, the model should be evaluated as competent for estimation of NPP at the regional level.

The work is part of a larger, ongoing effort to quantify and explain carbon budget dynamics in the grassland of Kazakhstan, a region where considerable knowledge gaps exist. Imminently, we are seeking to apply our model to the full spatial extent of grasslands in this country in order to quantify the long-term carbon change due to the significant reduction of anthropogenic impact during the transition time from the socialistic to liberal capitalistic economy after the collapse of the Soviet Union.

Acknowledgements

References

ALISOV, B.P., DROSDOW, O.A. and RUBINSTEIN, E.S., 1956, *Lehrbuch Der Klimatologie* (Berlin: VEB Deutscher Verlag der Wissenschaften).

ASRAR, G.M., FUCHS, M.M., KANEMASU, E.T. and HATFIELD, J.L., 1984, Estimating absorbed photosynthetically active radiation and leaf area index from spectral reflectance in wheat. *Agronomy Journal*, **87**, pp. 300–306.

BEGUE, A., DESPRAT, J.F., IMBERNON, J. and BARET, F., 1991, Radiation use efficiency of pearl millet in the Sahelian zone. *Agricultural and Forest Meteorology*, **56**, pp. 93–110.

BEHRENFELD, M.J., RANDERSON, J.T., MCCLAIN, C.R., FELDMAN, G.C., LOS, S.O. and TUCKER, C.J., 2001, Biospheric primary production during an ENSO transition. *Science*, **291**, pp. 2594–2597.

BROWN, L.J., CHEN, J.M., LEBLANC, S.G. and CIHLAR, J., 2000, Shortwave infra-red correction to the simple ratio: an image and model analysis. *Remote Sensing of Environment*, **77**, pp. 16–25.

CANEYE MANUALS, 2006, Can-Eye output variables. Definitions and theoretical background. Available online at: http://www4.paca.inra.fr/can-eye/Documentation-Publications/Documentation (accessed 17 July 2010).

FARTUSCHINA, M.M., 1986, *Produktivnost Senokosov I Pastbistch*, pp. 74–77 (Novosibirsk: Nauka) [in Russian].

FENSHOLT, R., SANDHOLT, I., RASMUSSEN, M.S., STISEN, S. and DIOUF, A., 2007, Evaluation of satellite based primary production modelling in the semi-arid Sahel. *Remote Sensing of Environment*, **105**, pp. 173–188.

FIELD, C.B., RANDERSON, J.T. and MALMSTRÖM, C.M., 1995, Global net primary production: combining ecology and remote-sensing. *Remote Sensing of Environment*, **51**, pp. 74–88.

FROUIN, R. and PINKER, R.T., 1995, Estimating photosynthetically active radiation (PAR) at the Earth's surface from satellite observations. *Remote Sensing of Environment*, **51**, pp. 98–107.

GILMANOV, T.G., 1996, NPP grassland: Shortandy, Kazakhstan, 1975–1980. Data set. Oak Ridge National Laboratory Distributed Active Archive Center, Oak Ridge, TN, USA. Available online at: http://www.daac.ornl.gov (accessed 3 September 2010).

GILMANOV, T.G., JOHNSON, D.A., SALIENDRA, N.Z., AKSHALOV, K. and WYLIE, B.K., 2004, Gross primary productivity of the true steppe in Central Asia in relation to NDVI: scaling up CO2 fluxes. *Environmental Management*, **33**, pp. 492–508.

GILMANOV, T.G., PATRON, W.J. and OJIMA, D.S., 1997, Testing the CENTURY ecosystem level model on data sets from eight grassland sites in the former USSR representing a wide climatic/soil gradient. *Ecological Modelling*, **96**, pp. 191–210.

GOWARD, S.N. and HUEMMRICH, K.F., 1992, Vegetation canopy PAR absorptance and the normalized difference vegetation index: an assessment using the SAIL model. *Remote Sensing of Environment*, **39**, pp. 119–140.

GOWARD, S.N., WARING, R.H., DYE, D.G. and YANG, J., 1994, Ecological remote-sensing at OTTER: satellite macroscale observations. *Ecological Applications*, **4**, pp. 322–343.

GOWER, S.T., KUCHARIK, C.J. and NORMAN, J.M., 1999, Direct and indirect estimation of leaf area index, FAPAR, and net primary production of terrestrial ecosystems. *Remote Sensing of Environment*, **70**, pp. 29–51.

GRISTCHENCO, O.M., 1972, Podzemnaya phytomassa pyreynych limanov i eye rol w biologitchesom krugovorote westchestv i energii. In *Materialy O Flore I Rastitelnosti Severnogo Pricaspiya*, pp. 54–68 (Leningrad: Wsesojuz. geogr. obstch.) [in Russian].

HEINSCH, F.A., Reeves, M. and Bowker, C.F., 2003, User's guide, GPP and NPP (MOD 17A2/A3) products, NASA MODIS land algorithm (Missoula, MT: University of Montana), p. 57.

HENEBRY, G.M., 2009, Carbon in idle croplands. *Nature*, **457**, pp. 1089–1090.

HILL, M.J., DONALD, G.E., HYDER, M.W. and SMITH, R.C.G., 2004, Estimation of pasture growth rate in the south west of Western Australia from AVHRR NDVI and climate data. *Remote Sensing of Environment*, **93**, pp. 528–545.

HOLBEN, B.N., 1986, Characteristics of maximum-value composite images from temporal AVHRR data. *International Journal of Remote Sensing*, **7**, pp. 1417–1434.

HOOKER, S.B., ESAIAS, W.E., FELDMAN, G.C., GREGG, W.W. and McCLAIN, C.R., 1992, *An Overview of SeawiFS and Ocean Color*, NASA Technical Memorandum 104566, vol. 1 (Washington, DC: NASA).

HUI, D. and JACKSON, R.B., 2006, Geographic and interannual variability in biomass partitioning in grassland ecosystems: a synthesis of field data. *New Phytologist*, **169**, pp. 85–93.

HUNT, E.R., KELLY, R.D., SMITH, W.K., FAHNESTOCK, J.T., WELKER, J.M. and REINERS, W.A., 2004, Estimation of carbon sequestration by combining remote-sensing and net ecosystem exchange data for northern mixed-grass prairie and sagebrush-steppe ecosystems. *Environmental Management*, **33**, pp. 432–441.

JINGUO, Y., ZHENG, N. and CHENLI, W., 2006, Vegetation NPP distribution based on MODIS data and CASA model: a case study of Northern Hebei province. *Chinese Geographical Science*, **16**, pp. 334–341.

JONCKHEERE, I., FLECK, S., NACKAERTS, K., MUYSA, B., COPPIN, P., WEISS, M. and BARET, F., 2004, Review of methods for in situ leaf area index determination. Part I. Theories, sensors and hemispherical photography. *Agricultural and Forest Meteorology*, **121**, pp. 19–35.

JUSTICE, C.O., TOWNSHEND, J.R.G., VERMOTE, E.F., MASUOKA, E., WOLFE, R.E., SALEOUS, N., ROY, D.P. and MORISETE, J.T., 2002, An overview of MODIS land processing and product status. *Remote Sensing of Environment*, **83**, pp. 3–15.

LAL, R., 2004, Carbon sequestration in soils of Central Asia. *Land Degradation & Development*, **15**, pp. 563–572.

LANG, A.R. and XIANG, Y., 1986, Estimation of leaf area index from transmission of direct sunlight in discontinuous canopies. *Agricultural and Forest Meteorology*, **35**, pp. 229–243.

Lioubimtseva, E., Cole, R., Adams, J.M. and Kapustin, G., 2005, Impacts of climate and land cover changes in arid lands of Central Asia. *Journal of Arid Environments*, **62**, pp. 285–308.

Long, S.P., Garsia, E. and Imbamba, S.K., 1989, Primary productivity of natural grass ecosystems of the tropics: a re-appraisal. *Plant & Soil*, **115**, pp. 155–166.

Lu, D., 2006, The potential and challenge of remote-sensing-based biomass estimation. *International Journal of Remote Sensing*, **27**, pp. 1297–1328.

Makarowa, L.I., 1971, Tyrsovaya formacia w basseyne ozera Tchelkar. In *Materialy Po Flore I Rastitelnosti Severnogo Prikaspiya*, pp. 179–186 (Leningrad: Wsesojuz. geogr. obstch.) [in Russian].

Mccoy, R.M. (Ed.), 2005, *Field Methods in Remote Sensing*, p. 23 (New York: The Guildford Press).

Monsi, M. and Saeki, T., 1953, Über den Lichtfaktor in den Pflanzengesellschaften und seine Bedeutung für die Stoffproduktion. *Japanese Journal of Botany*, **14**, pp. 22–52.

Monteith, J.L., 1972, Solar radiation and productivity in tropical ecosystems. *Journal of Applied Ecology*, **9**, pp. 747–766.

Monteith, J.L., 1977, Climate and efficiency of crop production. *Philosophical Transactions of the Royal Society of London, Series B*, **281**, pp. 277–294.

Monteith, J.L. and Unsworth, M., 1990, *Principles of Environmental Physics*, p. 291 (London: Arnold).

Muratova, N.R., 2007, *Annual Report of the Space Research Institute of the Science Academy of Kazakhstan*, pp. 61–72 (Almaty: Academic-Publishers).

Myneni, R.B., Nemani, R.R. and Running, S.W., 1997, Estimation of global LAI and fPAR from radiative transfer models. *IEEE Transactions on Geoscience and Remote Sensing*, **35**, pp. 1380–1393.

Myneni, R.B. and Williams, D.L., 1994, On the relationship between fAPAR and NDVI. *Remote Sensing of Environment*, **49**, pp. 200–211.

Perschina, M.N. and Yakovlewa, M.E., 1960, *Biologitcheskiy Krugovorot W Zone Sukhich Stepey SSSR. Dokl. Sov. Potchwowedov K VII Mezschdunar. Kongr. Potchwowedov W USA*, pp. 116–123 (Moscow: AN SSSR) [in Russian].

Pinzón, J.E., Pierce, J.F. and Tucker, C.J., 2001, Analysis of remote-sensing data using Hilbert-Huang transform. In *SCI 2001 Proceedings*, 22–25 July, Orlando, FL.

Potter, C.S., Randerson, J.T. and Field, C.B., 1993, Terrestrial ecosystem production: a process model based on global satellite and surface data. *Global Biogeochemical Cycles*, **7**, pp. 811–841.

Propastin, P. and Kappas, M., 2009a, Modelling net ecosystem exchange for grassland in Central Kazakhstan by combining remote-sensing and field data. *Remote Sensing*, **1**, pp. 159–183.

Propastin, P. and Kappas, M., 2009b, Mapping leaf area index in a semi-arid environment of Kazakhstan using fine-resolution satellite data and in situ measurements. *GIScience and Remote Sensing*, **46**, pp. 231–246.

Propastin, P. and Kappas, M., 2010, Modelling carbon sequestration in drylands of Kazakhstan using remote-sensing data and field measurements. In *Land Degradation and Desertification: Assessment, Mitigation and Remediation*, P. Zdruli, M. Pagliai, S. Kapur and A. Faz Cano (Eds.), pp. 297–306 (London: Springer).

Propastin, P., Kappas, M., Erasmi, S. and Muratova, N.R., 2007, Remote sensing based study on intra-annual dynamics of vegetation and climate in drylands of Kazakhstan. *Basic and Applied Dryland Research*, **2**, pp. 138–154.

Propastin, P.A., 2007, *Remote Sensing Based Study on Vegetation Dynamics in Dry Lands of Kazakhstan* (Stuttgart: Ibidem Publishers).

Reeves, M.C., Zhao, M. and Running, S.W., 2006, Applying improved estimates of MODIS productivity to characterize grassland vegetation dynamics. *Rangeland Ecology and Management*, **59**, pp. 1–10.

REICH, P.B., TURNER, D.P. and BOLSTAD, P., 1999, An approach to spatially distributed modelling of net primary production (NPP) at the landscape scale and its application in validation of EOS NPP products. *Remote Sensing of Environment*, **70**, pp. 69–81.

ROBERTS, M.J., LONG, S.P., TIESZEN, L.L. and BEADLE, C.L., 1993, Measurements of plant biomass and net primary production. In *Photosynthesis and Production in a Changing Environment: A Field and Laboratory Manual*, D.O. Hall (Ed.), pp. 1–21 (London: Chapman & Hall).

ROBINSON, S., MILNER-GULLAND, E.L. and ALIMAEV, I., 2002, Rangeland degradation in Kazakhstan during the Soviet-era: re-examining the evidence. *Journal of Arid Environments*, **53**, pp. 419–439.

RODIN, L.E., BAZILEVICH, N.T. and ROZOV, N.H., 1975, *Productivity of the World's Main Ecosystems*, pp. 13–26 (Washington, DC: National Academy of Sciences).

RUIMY, A., DEDIEU, G. and SAUGIER, B., 1994, Methodology for estimation of terrestrial net primary production from remotely sensed data. *Journal of Geophysical Research*, **99**, pp. 5263–5283.

RUIMY, A., JARVIS, P.G., BALDOCCHI, D.D. and SAUGIER, B., 1995, CO_2 fluxes over plant canopies and solar radiation: a review. *Advances in Ecological Research*, **26**, pp. 1–66.

RUIMY, A., KERGOAT, L. and BONDEAU, A., 1999, Comparing global models of terrestrial net primary productivity (NPP): analysis of differences in light absorption and light use efficiency. *Global Change Biology*, **5**, pp. 56–64.

RUNNING, S.W., BALDOCCHI, D.D., TURNER, D.P., GOWER, S.T., BAKWIN, P.S. and HIBBARD, K.A., 1999a, A global terrestrial monitoring network integrating tower fluxes, flask sampling, ecosystem modelling and Eos satellite data. *Remote Sensing of Environment*, **70**, pp. 108–127.

RUNNING, S.W., NEMANI, J.M., GLASSY, J.M. and THORNTON, P.E., 1999b, MODIS daily photosynthesis and annual net primary production (NPP) product (MOD17). Algorithm Theoretical Basis Document V.3.0. Available online at: http://ntsg.umt.edu/modis/MOD17UsersGuide.pdf (accessed 19 January 2010).

RUNNING, S.W., THORNTON, P.E. and NEMANI, R., 2000, Global terrestrial gross and net primary productivity from the Earth observing system. In *Methods in Ecosystem Science*, O.E. Sala, R.B. Jackson, H.A. Mooney and R.W. Howarth (Eds.), pp. 44–57 (New York: Springer).

RYCHNOVSKA, M., ULEHLOVA, B., JAKRLOVA, J. and TESAROVA, M., 1980, Biomass budget and energy flow in alluvial meadow ecosystem. In *Proceedings of the XIII International Grassland Congress Leipzig, Gdr*, E. Wojahn and H. Thöns (Eds.), pp. 473–475 (Berlin: Akademie).

SCURLOCK, J.M.O. and OLSON, R.J., 2002, Terrestrial net primary productivity – a brief history and a new world database. *Environmental Review*, **10**, pp. 91–109.

SEAQUIST, J.W. and OLSSON, L., 1999, Rapid estimation of photosynthetically active radiation over the West African Sahel using the Pathfinder Land data set. *Ecological Modelling*, **1**, pp. 205–213.

SEAQUIST, J.W., OLSSON, L. and ARDO, J., 2003, A remote-sensing-based primary production model for grassland biomes. *Ecological Modelling*, **169**, pp. 131–155.

SHATOKHINA, N.G., 1988, The authentic steppe of Kazakhstan, Tselinograd region. In *Biological Productivity of Herbaceous Ecosystems*, V.B. Ilyin (Ed.), pp. 32–42 (Moscow: Nauka) [in Russian].

SINGH, J.S., LAUENROTH, W.K. and STEINHORST, R.K., 1975, Review and assessment of various techniques for estimating net aerial primary production in grasslands from harvest data. *Botanical Review*, **41**, pp. 181–232.

SINGSAAS, E.L., OOR, D.R. and DE LUCIA, E.N., 2001, Variation in measured values of photosynthetic quantum yield in ecophysiological studies. *Oecologia*, **128**, pp. 15–23.

TESAROVA, M. and GLOSER, J., 1976, Total CO_2 outputs from alluvial soils with two types of grassland communities. *Pedobiologia*, **16**, 364–372.

TITLYANOVA, A.A., 1988, Productivnost' travianykh ekosistem. In *Biologicheskaia Produktivnost' Travianykh Ekosistem*, B.B. Ilyin (Ed.), pp. 109–127 (Moscow: Nauka) [in Russian].

TUCKER, C.J., DESCLOITRES, J., FELDMAN, G. and FRANZ, B., SeaWiFS global land data set for 1997–2002 (in press).

TURNER, D.P., URBANSKI, S., BREMER, D., WOFSY, S.C., MEYERS, T., GOWER, S. and GREGORY, M., 2003, A cross-biome comparison of daily light use efficiency for gross primary production. *Global Change Biology*, **9**, pp. 383–395.

TYURMENCO, A.N., 1975, Biologitcheskiy krugovorot zolnych elementov pod celinnoy i culturnoy rastitelnostyu w zone sukhich i polupustynnych stepey. In *Genesis, Swoystwa I Plodorodiye Potchw*, pp. 135–176 (Kazan': Izd. Kazan. Universiteta) [in Russian].

WEISS, M., BARET, F., SMITH, G.L., JONCKHEERE, I. and COPPIN, P., 2004, Review of methods for in situ leaf area index determination. Part II. Estimation of LAI, errors and sampling. *Agricultural and Forest Meteorology*, **121**, pp. 37–53.

WHITE, M.A., THORNTON, P.E., RUNNING, S.W. and NEMANI, R.R., 2000, Parameterisation and sensitivity analysis of the BIOME-BGC terrestrial ecosystem model: net primary production controls. *Earth Interactions*, **4**, pp. 1–85.

XIAO, X., HOLLINGER, D., ABER, J., GOLTZ, M., DAVIDSON, E.A., ZHANG, Q. and MOORE, B., 2004, Satellite-based modelling of gross primary production in an evergreen needleaf forest. *Remote Sensing of Environment*, **89**, pp. 519–534.

YUAN, L., LIANGLIN, W. and CUI, H., 2008, Estimation of net primary productivity in North Tibet Plateau by integrating CASA model with MODIS data. In *Geoinformatics 2008 Joint Conference on GIS and Built Environment*. L. Liu, X. Li, X. Zhang and Y. Lao (Eds.), *Proceedings of SPIE*, Vol. 71450, 3 November 2008 (Bellingham, WA: SPIE – Society of Photo Optical Instrumentation Engineers).

ZHANG, D., HUI, D., LUO, Y. and ZHOU, G., 2008, Rates of litter decomposition in terrestrial ecosystems: global patterns and controlling factors. *Journal of Plant Ecology*, **1**, pp. 85–93.

ZHENG, D., PRINCE, S. and WRIGHT, R., 2003, Terrestrial net primary production estimates for 0.5° grid cells from field observations – a contribution to global biogeochemical modelling. *Global Change Biology*, **9**, pp. 46–64.